Exoplanet Detection via Transit Photometry

Department of Physics, University of California, Santa Barbara, CA 93106
(Dated: June 13, 2023)

Transit Photometry provides a promising and reliable way to detect exoplanets by observing dips in luminosity of stars. It has the potential to detect exoplanets that may be habitable for humans in the future as demonstrated by the MEarth Project. In this paper, we attempt to detect two transiting exoplanets Gliese 1214 b and Wasp 14 b. We find evidence of a magnitude dip for Wasp 14 implying the transit of an exoplanet. Whereas, the data for Gliese 1214 provided issues- making this attempt unsuccessful. We discuss reasons as to why one observation worked while the other did not.

INTRODUCTION

In 1992, astronomers Alex Wolszczan and Dale Frail discovered two exoplanets. In their research, they used a 305-m Arecibo radiotelescope to make precise timing measurements of pulses from a pulsar (a rapidly rotating neutron star) [1]. Through observation, there turned out to be two or more planets orbiting the pulsar- becoming the first proof of the existence of exoplanets. Since then, a new branch of physics focusing on the study of exoplanets has emerged, leading to the observation of numerous additional exoplanets. Innovative approaches to detect exoplanets beyond the pulsar timing method developed, including methods like Direct Imaging, Gravitational Microlensing, and the Doppler Method. All these methods work best and excel in different scenarios, but in this paper, we will look to another method that observes the magnitude of a star over time. If a dip in magnitude is observed, it can be possible that an exoplanet contributed to the light loss[2].

Transit Photometry Method

The Transit Photometry method depends on taking the light flux of the target star and comparing these values to other stars in the same within the same image [3]. Using these images, a data set of flux values is generated for each frame captured during the observation session [3].This method does have its limits as there is a dependence on orientation of the transiting exoplanet relative to earth, so it would be improbable of detecting an exoplanet from a random star system [4]. Furthermore, the effectiveness of this method depends on the ability to establish detection thresholds to control any potentially false discoveries attributed to background noise or statistical error[5]. These are all important considerations for when picking a target and conducting analysis on the data.

Aperture Photometry

This photometry is usually done with a digital Charged Couple Device (CCD) on earth that can determine the stellar magnitudes of calibrated observation stars [6]. Aperture Photometry employs CCD in by setting an aperture around the perimeter of the target star and one larger surrounding the area of the target star [3]. This accounts for uncertainties of magnitude within the stars region.

Advancements in technology have improved the resolution, accuracy, and capabilities of telescopes. For instance, the James Webb Space Telescope launched December 25, 2021, enables more precise measurements and study more distant exoplanets. One method of studying exoplanets on the James Webb Space Telescope is Transit Photometry. As humanity progresses and technology advances, the ongoing research in the field of exoplanet discovery holds the potential to address fundamental questions in the future. These include what exoplanet may be the most suitable for human life? or whether intelligent life exists beyond earth?

In this paper, we will attempt to apply the transit photometry method to two stars with known exoplanets GJ-1214 b and WASP-14 b. Los Cumbres Observatory (LCO) Visibility Tool[7], alongside the NASA Exoplanet Watch Target List [8] were used to pick our targets.

EXOPLANET TARGETS AND OBSERVATIONS

A. GJ-1214b

Discovered in December 2009, GJ-1214b was part of a project known as MEarth, which utilized automated telescopes to observe M-dwarf stars through Transit Photometry[9]. In the project, M-dwarf stars were chosen to increase the probability of finding the existence of Earth-like exoplanets. GJ-1214b is a super-Earth exoplanet orbiting an M-type star, GJ-1214 (seen in fig. 2). GJ-1214 b is observed to have a mass $6.55M_{Earth}$, a radius $2.68R_{Earth}$ with a 1.58-day orbit [9]. Ice giants typically have a range of radius $2R_{Earth}$ to $6R_{Earth}$, making GJ-1214b an intermediary between Earth and ice giants- hence a super-earth. [9].

The suitability of GJ-1214 as a candidate for transit photometry arises from the characteristics of M-dwarf stars. These stars are typically dim enough to prevent telescope saturation, and their relatively smaller size allows for the easier detection of transiting planets. The feasibility of observation is first evaluated by calculating the "Signal to Noise Ratio," or SNR. The SNR provides a measure of the quality of a target's signal against the background noise. This is most important for Transit Photometry as we would need a high SNR for better quality to observe any dip

FIG. 1. FROM OUR DATA: Raw image of the GJ-1214 star centered on the image displayed using a .fits visualization tool

in magnitudes. Furthermore, the SNR will also tell us the feasibility of observation using the available Los Cumbres Observatory telescopes. Identifying a star with a large transit depth is particularly important because, in the event of telescope saturation, a large transit depth can compensate. The SNR of GJ-1214 star is calculated using its apparant magnitude of 14.71 and exposure time using the LCO calculator [7]. The exposure time is the integration time times the number of exposures. The SNR of the star is 680.5.

The signal to noise ratio of an exoplanet orbiting a star is roughly...

$$\frac{S}{N}_{exoplanet} = \delta \times \frac{S}{N}_{star} \tag{1}$$

Where the transit depth is

$$\delta = \frac{R_{planet}^2}{R_{star}^2} \tag{2}$$

The radius of GJ-1214 is $R_{star} = 0.216 \pm 0.012 R_S$ where R_S is the radius of the sun and radius of GJ-1214 b $R_{planet} = 0.24463 \pm 0.00473 R_J$ where R_J is the radius of Jupiter[10]. The calculated SNR of 8.83.

We assigned Los Cumbres Cerro Tololo Observatory on May 8, 2023: 12:30 am - 2:30 am UTC to observe the transit of GJ-1214 b. Our data set comprises of 360 exposures with an integration time of 10 seconds. For this observation, the 0.4-meter Telescope was equipped with an SDSS-i' filter and directed towards the following coordinates: Right Ascension 17:15:18.9 and Declination +04:57:50.06. The use of the Sloan Digital Sky Survey infrared filter is based on the fact that GJ-1214b orbits an M-dwarf star, which exhibits a dimmer luminosity and operates at temperatures ranging from 2,000 to 3,500 K. As a result, the majority of its radiation falls within the infrared range of the electromagnetic spectrum. The SDSS-i' captures wavelengths of about 762.5 nm in the near-infrared range [11]. The observation request is seen below:

Target Name	RA (J2000)	Dec (J2000)	Filter	# Exposures	Integration Time (s)	Observational Windows
GJ-1214b	17:15:18.9	+04:57:50.06	SDSS-i'	360	10	May 8, 2023: 12:30 am - 2:30 am (UTC) (South America)

B. WASP-14b

Discovered in 2008 using Transit Photometry, WASP-14b is a gas-giant exoplanet orbiting an F-type star, WASP-14 (seen in Figure 2) [12]. It is observed to have a mass of $7.3 M_{Jupiter}$, planet radius of 1.28 R_{Jup} and a 2.24-day orbit

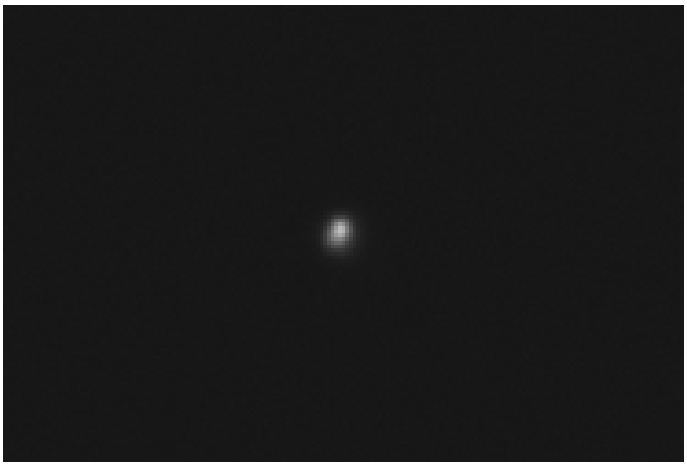

FIG. 2. FROM OUR DATA: Raw image of the WASP-14 star centered on the image displayed using a .fits visualization tool

[13]. Since WASP-14b is an irradiated hot-jupiter, observations may involve significant levels of incident flux, slow rotation, and the possibility of substantial temperature variations [14].

Again, the suitability of WASP-14 b as target for Transit photometry (or any other exoplanet) is dependent on the SNR. It is important to note that given the telescopes, the best way to maximize success is to find a star with a large transit depth. Fortunately, WASP-14 b is a large planet. This leads us to the SNR calculation of the planet. The radius of WASP-14 is $1.306R_{Sun}$ and radius of wasp 14 b is $1.281R_J$ where R_J is the radius of Jupiter [10]. The SNR of Wasp-14 star was calculated using its apparent magnitude of 9.75 and exposure time of 10 sec in the LCO calculator [7]. Again, The exposure time is the integration time times the number of exposures. The SNR of the star is 10446.9. Using equations 1.) and 2.), we find the SNR of WASP-14 b to be 101.45.

We assigned Los Cumbres Observatory on May 17, 2023: 11:30 – 16:30 UTC- North America to observe the transit of WASP-14 b. Our data set consists of 360 exposures and an integration time of 10 seconds. For this observation, a 0.4-meter telescope was assigned with SDSS-g' filter towards the following coordinates: Right Ascension 14:33:06.0 and Declination +21:53:41. THE SDSS filter choice is based on WASP-14 b orbiting an F-type star which are larger than G-type stars like our sun. F-type stars tend to be within 6,000–7,400 K and as a result, emit a large amount of radiation within the green visible spectrum. The SDSS-g' filter captures wavelengths around 477.0 nm making it a good choice [11]. The observation request is seen below:

Target Name	RA (J2000)	Dec (J2000)	Filter	# Exposures	Integration Time (s)	Observational Windows
WASP-14b	14:33:06.0	+21:53:41	SDSS-g'	360	10	May 17, 2023: 11:30 am - 16:30 am (UTC) (North America)

[]

METHODS

To perform photometry on the images, Python is employed using the open-source "astropy" package used to import and extract data from the .fits formatted banzai images provided by LCO. Additionally, the Photutils package is used for two essential functions. First, to help in detecting sources within the images, photutils.detection function is necessary. This tool will be used to conduct background estimation by subtracting the background noise from an image. Secondly, to perform aperture photometry, the photutils.aperture function is included. This tool will be used to create circular apertures around sources.

The first step is to find the number of stars, and their x and y coordinate positions in a single banzai image. We specifically chose an image pre-transit for precaution. The image is initially presented using a gray-scale color map, where a logarithmic transformation of the image data is applied to enhance the visibility of pixel variations.

Following this, a sigma clip is used to exclude values 3.0 standard deviations away. A sigma clip is used in statistics to exclude outliers from a data set, in this case it is used as background estimation to exclude bright sources. The

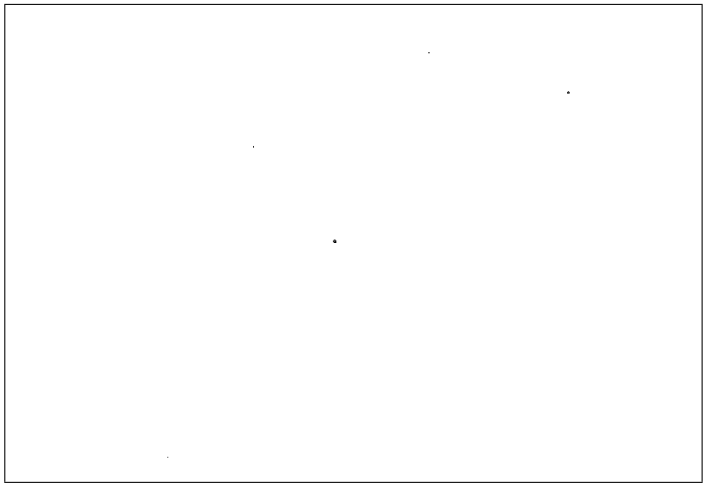

FIG. 3. Gray-scale image of WASP-14 b data. Our target star is seen in the center.

function MedianBackground() is employed due to its robustness to outliers and image noise. To identify smaller and fainter sources in the image, the DAOStarFinder algorithm from Photutils is also used. The gaussian kernel's full width at half maximum (FWHM) is set to 5, accompanied by a threshold of 5σ. The threshold is an important step as it helps determines what is considered as a source (or star) in the banzai image. Reducing the threshold may include more sources. The photon count for each source is obtained by using a circular aperture tool with a radius of 15 pixels. The sources are all plotted with visible circular apertures. A .csv file containing all star positions and aperture sums is created. The resultant images for both GJ-1214 b and WASP-14 b are seen in Figure 4 and Figure 5.

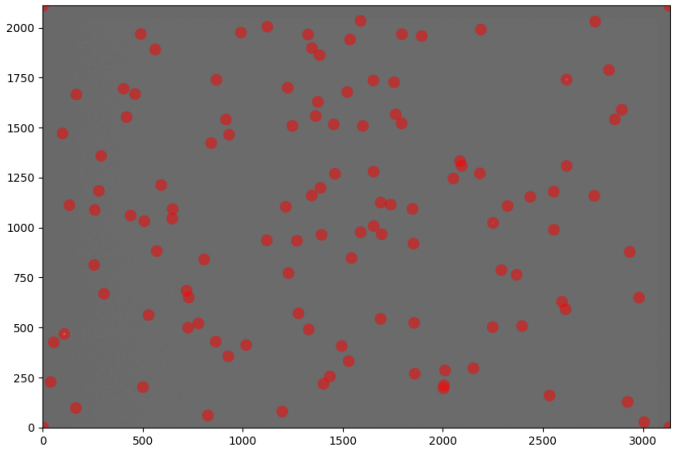

FIG. 4. 117 sources were identified using the DAOStarFinder tool from Photoutils for GJ-1214b

Next, the data from all banzai image frames of our stars are extracted. Aperture photometry is performed on each source with a radius of 15 pixels using the same functions as before. Using AstroArt with online data, we are able to identify our target star hosting our exoplanet. Since we are looking to only perform photometry on our target star, we define its position in the code. Background data is estimated using the "Background2D" function with a specified box size of (50, 50) and a filter size of (3, 3). The box size determines the region in which background estimation will occur, whereas, the filter size how much the background estimation will be applied to the image. After subtracting the background data, we can proceed with aperture photometry. Using the circular aperture tool with a radius of 15 pixels, the respective aperture sums and positions are collected for each frame. Accuracy is determined by using a calibration tool that calculates and calibrates the median value of our target star's magnitude. Here, we use "calibrator." A plot of the apparent magnitude of our target star is created. Frames on the x-axis and the normalized calibrated magnitudes on the y-axis.

Finally, numerous stars are calibrated and weighted against their median values. A variability check is completed

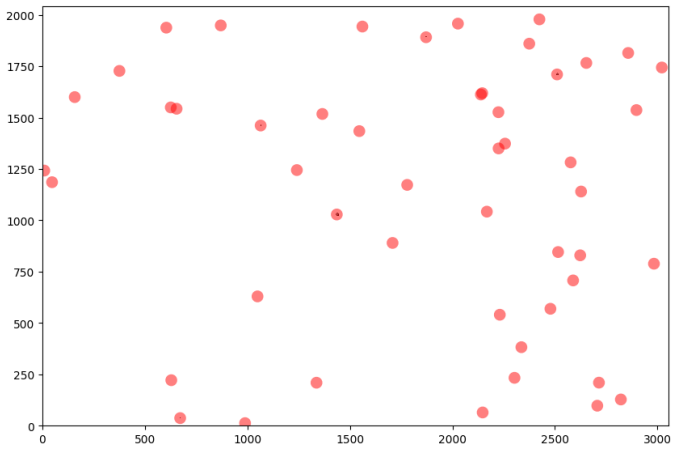

FIG. 5. 50 sources were identified using the DAOStarFinder tool from Phototulis for WASP-14

to filter out calibrated stars that exhibit significant variability in their weighted magnitudes. The remaining stars, which pass the variability check, are used to generate a light curve with our target star. A separate light curve of our target star is plotted with the average calibration light curve. This provides a comparison is essential to evaluate our target star's brightness variations relative to other stars.

RESULTS

C. GJ-1214 b

We did not obtain suitable results from GJ-1214 b. An in-depth explanation of what went wrong with this data set will be in the "Discussion" section.

Error Analysis for GJ-1214 b

A combination of systematic and statistical error contributed to the failure of observing transit in the data. The 0.4m telescope with the sdss i filter was not the best telescope to observe GJ-1214 b. The telescope saturates with SNR's below 700. This error is most apparent in GJ-1214 b for its low signal to noise ratio. Background noise and loss of data due to saturation made it so that there were no dips in magnitudes to be observed. Preliminary calculations showed that any magnitudes would fluctuate up to an order of 10.

D. WASP-14 b

The plot of of the calibrated magnitudes for our target star, WASP-14 is seen in Figure 6. The initial blue line is an approximation of where the Transit of WASP-14 b begins- approximated to be around 110 frames. The following blue lines highlight the large dip in magnitude between 260 - 325 frames. From this plot, it is visible that WASP-14 experiences a dip in magnitude of about 0.8. Furthermore, the drastic vertical dips present at around 160 frames and 280 frames are attributed to outlier stars.

The plot of stars calibrated and weighted against their median values alongside WASP-14 are seen in Figure 7 and Figure 8. Again, we see a dip in magnitude from about between 260 - 325 frames. The dip in brightness of the star can be attributed to the WASP-14 b exoplanet passing by the star.

Error Analysis for WASP-14 b

To address for the statistical error present in our WASP-14 b data,we perform error analysis on the light curves generated using Python. The error in our data is determined by taking the standard deviations of our target star

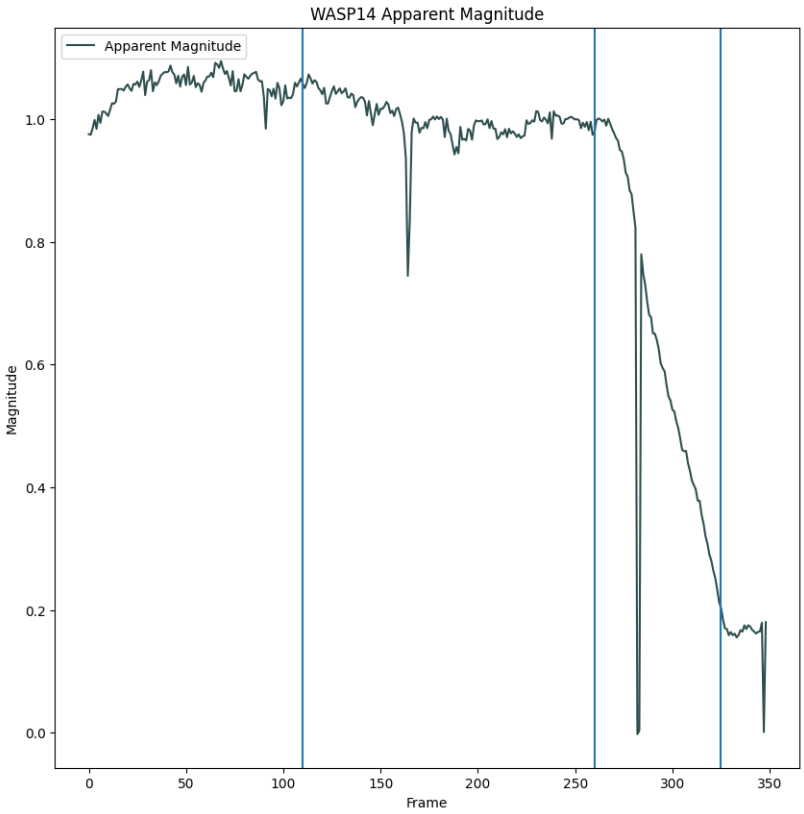

FIG. 6. Plot of normalized calibrated magnitudes over each frame.

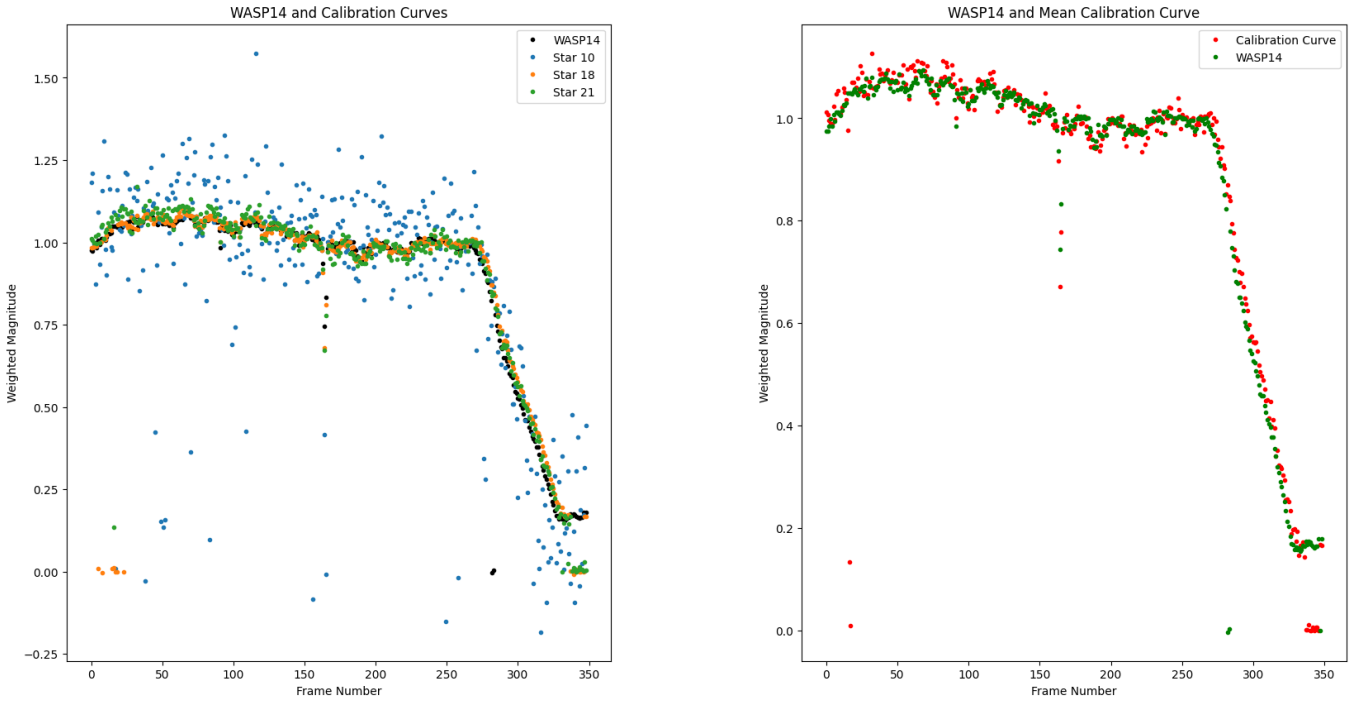

FIG. 7. The left plot displays a light curve of our target star is plotted with the stars that passed the variability check. The right plot displays the light curve of our target star plotted with the average calibration light curve

before transit. A "static frames" functions to identify all images prior to transit, and the corresponding magnitudes are stored in an array. The magnitudes recorded before transit are averaged, and are weighted differences from the mean. Statistical measurements on the magnitudes completed:

$$\overline{x} = 0.9889874677498032$$
$$\sigma = 0.016766369785125673$$
$$S = 0.00028111115577157507$$

These values represent the mean, standard deviation, and variance, respectively. After eliminating magnitude outliers and including the standard deviation as the uncertainty for each data point, the data is plotted seen in Figure 8. The statistical error is to be attributed to a combination of background noise, and error with the background estimation from the photutils package. Error also presents itself with the tools we used. The 0.4m telescope with the sdss g filter for WASP-14 b presents issues considering that the SNR's for the exoplanet is below 700. The telescope saturates below that range, leading to a loss of information. This did not affect the WASP data as much as the GJ-1214 data.

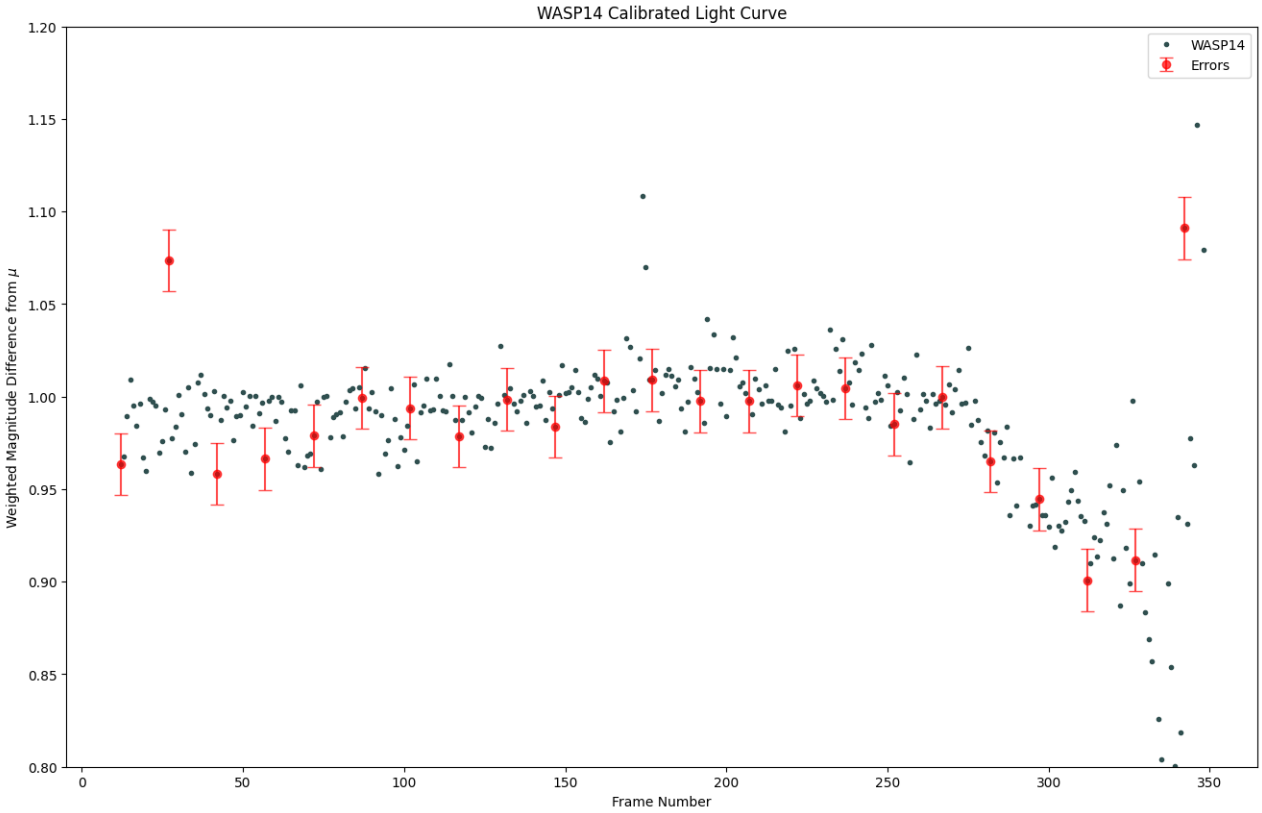

FIG. 8.

DISCUSSION

In this paper, we observe a dip in magnitude for one of the two target stars implying the existence of an exoplanet. GJ-1214 b was not successful for a multitude of reasons. We were directed to go for an M-type star(GJ-1214) due to it's low luminosity, but this presented issues in combination with the low SNR. A low SNR means the background nose flushed out the signal. If we were to re-attempt Transit Photometry for GJ-1214, we would look to find telescopes that do not saturate at lower SNR's. This can also be done by changing the exposures and integration time of the observation request. With thi improved telescope equipment, we would re-attempt WASP-14 with more observation time towards the tail end of the transit. We did not have enough observation time to observe the full transit. With the added end-of-transit data, we can fit a square wave model onto the graph and obtain an accurate and precise measurements of how much the magnitude dipped. Furthermore, we can use this data to calculate transit depth and estimate characteristics of the exoplanet. The characteristics of exoplanets are essential information for the future of

humanity. Following the steps of the MEarth project, finding habitable planets for humans may also mean a habitable planet for intelligent life forms beyond humans- fulfilling human curiosity and inquisitive nature.

ACKNOWLEDGEMENTS

I would like to thank Samuel Whitebook for his help and guidance through the Transit Photometry code he has provided for us to use. I would also like to extend a thanks to our TA Jeonghwa Kim for the assistance in submitting the observation requests and making adjustments to allow us to get the best data possible.

[1] A. Wolszczan and D. A. Frail, Nature **355**, 145 (1992).
[2] T. P. Society, "Down in front!: The transit photometry method," (2023).
[3] D. Afanasev, "Detection of exoplanets using the transit method," (2018), arXiv:1803.05565 [physics.gen-ph].
[4] H. J. Deeg and R. Alonso, in *Handbook of Exoplanets* (Springer International Publishing, 2018) pp. 633–657.
[5] J. M. Jenkins, D. A. Caldwell, and W. J. Borucki, The Astrophysical Journal **564**, 495 (2002).
[6] K. Mighell, in *Precision CCD Photometry*, Vol. 189 (1999) p. 50.
[7] L. C. O. (LCO), "Visibility tool," (2023).
[8] NASA, "Exoplanet watch," (2023).
[9] D. Charbonneau, Z. K. Berta, J. Irwin, C. J. Burke, P. Nutzman, L. A. Buchhave, C. Lovis, X. Bonfils, D. W. Latham, S. Udry, R. A. Murray-Clay, M. J. Holman, E. E. Falco, J. N. Winn, D. Queloz, F. Pepe, M. Mayor, X. Delfosse, and T. Forveille, Nature **462**, 891 (2009).
[10] E. Exoplanet, "Planetary catalog," (2023).
[11] S. D. S. Servers, "Sdss filters," (2023).
[12] Y. C. Joshi, D. Pollacco, A. C. Cameron, I. Skillen, E. Simpson, I. Steele, R. A. Street, H. C. Stempels, D. J. Christian, L. Hebb, F. Bouchy, N. P. Gibson, G. Hé brard, F. P. Keenan, B. Loeillet, J. Meaburn, C. Moutou, B. Smalley, I. Todd, R. G. West, D. R. Anderson, S. Bentley, B. Enoch, C. A. Haswell, C. Hellier, K. Horne, J. Irwin, T. A. Lister, I. McDonald, P. Maxted, M. Mayor, A. J. Norton, N. Parley, C. Perrier, F. Pont, D. Queloz, R. Ryans, A. M. S. Smith, S. Udry, P. J. Wheatley, and D. M. Wilson, Monthly Notices of the Royal Astronomical Society **392**, 1532 (2009).
[13] S. Raetz, G. Maciejewski, M. Seeliger, C. Marka, M. Fernández, T. Güver, E. Göğüş, G. Nowak, M. Vaňko, A. Berndt, T. Eisenbeiss, M. Mugrauer, L. Trepl, and J. Gelszinnis, Monthly Notices of the Royal Astronomical Society **451**, 4139 (2015), https://academic.oup.com/mnras/article-pdf/451/4/4139/3886180/stv1219.pdf.
[14] I. Wong, H. A. Knutson, N. K. Lewis, T. Kataria, A. Burrows, J. J. Fortney, J. Schwartz, E. Agol, N. B. Cowan, D. Deming, J.-M. Désert, B. J. Fulton, A. W. Howard, J. Langton, G. Laughlin, A. P. Showman, and K. Todorov, The Astrophysical Journal **811**, 122 (2015).